PHYSICAL REVIEW B VOLUME 32, NUMBER 12 15 DECEMBER 1985

# Electronic structure of crystalline and amorphous silicon dioxide

Raju P. Gupta
*Section de Recherches de Métallurgie Physique, Centre d'Etudes Nucléaires de Saclay, 91191 Gif-Sur-Yvette Cedex, France*
(Received 21 June 1985)

The electronic structure of $\alpha$-quartz and $a$-$SiO_2$ has been calculated using the tight-binding recursion method. For $a$-$SiO_2$ two structural models were used. The first one consisted of the continuous-random-network model constructed by Bell and Dean (BD). The second model was generated by Doan from molecular-dynamics (MD) simulations by quenching the liquid $SiO_2$ to room temperature. While the bond-length distortions in the BD model are small from the values in $\alpha$-quartz, the MD model yields relatively large distortions. Our calculations show that the electronic structures of $\alpha$-quartz and $a$-$SiO_2$ are, roughly speaking, quite similar. The valence band can be divided into three parts. A narrow band $\sim$2.5 eV wide at $\sim -20$ eV is dominated by the O 2$s$ states. This band is separated by a gap from the silicon-oxygen bonding states. The top of the valence band is formed essentially of nonbonding oxygen states approximately 4 eV in width. A region of low densities of states separates the bonding-nonbonding states which have a width of 11.5—13 eV. The results for BD model are quite close to those for $\alpha$-quartz but the MD model shows quantitative differences. In particular the bonding-nonbonding states have a slightly reduced bandwidth (11.5 eV compared to 13.0 eV in $\alpha$-quartz and BD model) and the valley between the nonbonding and bonding states is shallower. The valence-band edge remains unchanged by disorder but the conduction-band edge moves down, thus slightly reducing the band gap from 8.4 eV in $\alpha$-quartz to 7.5 eV in BD model and 7.2 eV in the MD model. We find effective charges of approximately 1.6 and 7.2 electrons at Si and O sites, respectively. A detailed analysis of the composition of the densities of states is presented and comparison with experimental data on x-ray emission, photoelectron spectra, and reflectivity made. The generally good agreement found between the experimental data and the MD model seems to indicate a large bond-length variation in amorphous silicon dioxide.

## I. INTRODUCTION

Silicon dioxide is a material of very considerable technological importance, including its use in microelectronic devices containing metal-oxide—semiconductor transistors, optical fibers, etc. It also forms the basis of the glass matrix for stocking the radioactive waste material. It exists in many crystalline forms, the better known being quartz, cristobalite, tridymite, stishovite, and coesite, but its best-known form is its amorphous state, called the amorphous silicon dioxide. This is also the form which can be fabricated in the purest state and is the most used technologically. With the exception of stishovite, which is a rare form of $SiO_2$, the basic structural unit in all the forms of $SiO_2$ is the same, an $SiO_4$ tetrahedron. Each silicon atom is tetrahedrally coordinated with four oxygen atoms and each oxygen atom serves as a bridge connecting two tetrahedra. The various forms of $SiO_2$ are obtained by linking the tetrahedra together in different ways. The two forms which are the most common and the most studied are the crystalline $\alpha$-quartz and the amorphous $a$-$SiO_2$. These are also the forms which are quite close together. In $\alpha$-quartz the Si—O bond length is 1.61 Å and the Si—O—Si angle 144°.[1] In $a$-$SiO_2$ these two parameters have a random distribution, but their mean values are about the same as in $\alpha$-quarts. The tetrahedron, on the other hand, remains almost perfect with only a very small deviation in $a$-$SiO_2$ in the O—Si—O angle of 109.5° in $\alpha$-quartz.[2]

There has been an extensive amount of experimental work on $SiO_2$ in order to gain insight into its electronic structure. This includes measurements of x-ray-emission and -absorption spectra,[3–6] x-ray (XPS) and ultraviolet (UPS) photoelectron spectra,[7–13] low-energy-electron energy-loss spectra,[14] photoconductivity,[15] optical reflectivity;[16,17] etc. From the photoconductivity measurements[15] a band gap of 8.9 eV has been deduced for $a$-$SiO_2$, and a comparison of the XPS data[9] for $a$-$SiO_2$ and $\alpha$-quartz shows the band gap in $\alpha$-quartz to be $\sim$0.5 eV larger than in $a$-$SiO_2$. On the other hand, the reflectivity spectra of $a$-$SiO_2$ and $\alpha$-quartz are quite similar,[16] which indicates that overall the electronic structures of $a$-$SiO_2$ and $\alpha$-quartz are quite similar.

For a detailed understanding of the electronic structure of $SiO_2$ and the changes brought by disorder, it is clear that the theoretical calculations of its electronic structure are indispensable. This has posed problems, however, since, first, topological disorder is difficult to take into account in an accurate first-principles calculation and this has limited the work on $a$-$SiO_2$, and, second, even in the crystalline forms the crystal structures of $SiO_2$ are quite complex, making detailed band-structure calculations quite cumbersome. As a result early theoretical work was based almost exclusively on molecular cluster models,[18–24] where the lattice is ignored and clusters of various sizes are used instead. The results from these calculations have been used to interpret experimental data on both $\alpha$-quartz and $a$-$SiO_2$. The basic problem with the

 

cluster methods is, however, the accuracy since the results strongly depend upon the size of the cluster, and the convergence is poor as the size of the cluster is increased. Within the last ten years band-structure calculations have been performed on $\beta$-cristobalite by Ciraci and Batra[25] and by Pantelides and Harrison,[26] on cristobalite, $\alpha$-quartz, and stishovite by Fowler and co-workers,[27–29] and on $\alpha$-quartz by Chelikowsky and Schlüter.[30] Fowler and co-workers calculated the energy bands at a few symmetry points, which allowed them to take advantage of group theory in diagonalizing their matrices. A tight-binding procedure using either the O $2s$ or O $2p$ orbitals was then used to interpolate the valence bands at other points in the Brillouin zone. Chelikowsky and Schlüter (CS) used the empirical pseudopotential method for $\alpha$-quartz which is hexagonal. This calculation was self-consistent and was performed on a small mesh of 16 points in the irreducible part of the Brillouin zone to obtain the densities of states (DOS's) and joint densities of states (JDOS's).

For $a$-$SiO_2$ two types of approaches have been pursued. Ching[31] has used a non-self-consistent linear combination of atomic orbitals (LCAO) method in conjunction with a cubic supercell containing approximately 160 atoms. The amorphous solid is thus composed of the periodic repetition of these cubic crystallites. The models for $a$-$SiO_2$ were constructed by taking three existing models[32–34] for $a$-Si, inserting oxygen atoms between each pair of silicon atoms, and then rescaling the atomic coordinates and the size of the cubic cell so that the density of $a$-$SiO_2$ is reproduced. The models were then relaxed using a Keating-type potential[35] to reduce the bond distortion. A minimal basis set was used for the electron eigenfunctions which resulted in a matrix $\sim 650 \times 650$ to be diagonalized. The densities of states and other quantities were obtained from a single point $\Gamma$ in reciprocal space. The merit of this work is that it is a first-principles calculation for $a$-$SiO_2$, but a minimal basis set is a severe constraint for a first-principles calculation. The second approach[36,37] is based on the cluster-Bethe-lattice (CBL) model where a small cluster representing the environment of the amorphous material is embedded in a Bethe lattice. Since the calculation becomes quite complicated with the increasing size of the cluster only small clusters are used. The interaction parameters are taken from a tight-binding fit, but the fluctuations in the parameters inherent in an amorphous solid due to disorder are ignored. The CBL model is a good technique for the study of amorphous solids, but it is clear that it can by no means represent an actual amorphous solid.

While these theoretical investigations have contributed significantly to our understanding of the electronic structure of $SiO_2$, a detailed study of the effect of disorder on the bonding properties of $SiO_2$ is still lacking and is timely. The tight-binding recursion method[38] is a technique which is ideally suited for this purpose. Since it is a real-space technique it does not require any periodic structure and is as easily applied to amorphous solids as it is to crystalline solids.[39] It takes fully into account the atomic coordinates of the amorphous network as long as these coordinates are known in advance and there is no inherent difficulty in using as many as 500—1000 atomic positions in an amorphous network without an excessive use of computer memory or time. As in the CBL model the calculation requires a knowledge of the tight-binding parameters, but unlike in the CBL these parameters can be made to fluctuate to reflect the disorder in the local environment around an atom. The advantage of a parametrized tight-binding model is that these parameters are usually obtained from a fit to an existing first-principles self-consistent calculation or from a fit to the experimental data. These parameters are thus *effective* parameters and are bound to be different from those obtained using true atomic wave functions, as was first pointed out by Slater and Koster.[40] A parametrized tight-binding model therefore does not suffer from the drawbacks of a minimal-basis-set LCAO calculation. In this paper we present the results of our electronic-structure calculation for $\alpha$-quartz and $a$-$SiO_2$ using the tight-binding recursion method. As was stated above, $\alpha$-quartz and $a$-$SiO_2$ are structurally very close together, and a detailed comparative study of the electronic structure of the two compounds therefore allows us to shed some light on the major effects of disorder on the bonding in $SiO_2$. We note here that a calculation of the electronic structure of $SiO_2$ by the tight-binding recursion method was presented recently by O'Reilly and Robertson,[41] but that work was concerned only with $\alpha$-quartz and uses a small cluster of 273 atoms. Furthermore, a detailed comparison with experimental data was not made.

The plan of this paper is as follows. In Sec. II the details of the calculation are described, including models which were used to represent the $a$-$SiO_2$. In Sec. III the results of our electronic-structure calculations are presented for $\alpha$-quartz and $a$-$SiO_2$, including a detailed analysis of the local DOS on silicon and oxygen sites and a further decomposition into $s$ and $p$ components. Section IV is devoted to a comparison with the experimental optical spectra, and concluding remarks are given in Sec. V.

## II. DETAILS OF CALCULATION

The crystal structure of $\alpha$-quartz is hexagonal and has three molecules of $SiO_2$ per unit cell. In our calculation the lattice parameter and the atomic coordinates were taken from Wyckoff.[1] In this structure a silicon atom is tetrahedrally surrounded by four oxygen atoms and an oxygen atom forms a bridge between two silicon atoms. Thus a Si atom has four O atoms as nearest neighbors and four Si atoms as next-nearest neighbors. An oxygen atom has two silicons as nearest neighbors and six oxygens as next-nearest neighbors, three each from the two tetrahedra to which the oxygen atom forms a bridge. The tetrahedron of oxygen atoms around a silicon atom is almost regular with Si—O bond length of 1.61 Å and oxygen-oxygen distances ranging between 2.60 and 2.67 Å. The silicon-silicon separation in $\alpha$-quartz is much larger (3.06 Å) than in a silicon crystal (2.36 Å).

For $a$-$SiO_2$ two models were chosen. The first, which will be denoted henceforth $a$-$SiO_2$ (BD), is the continuous-random-network distribution of Si and O atoms obtained by Bell and Dean.[42] This model contains

a total of 614 atoms in the cluster. In this model the $SiO_4$ tetrahedra are preserved in the interior of the cluster. The Si—O bond lengths and Si—O—Si bond angles, however, vary. The Si—O bond length has a mean value of 1.6 Å and a root-mean-square (rms) deviation of 3.5%, while the Si—O—Si bond angle has a mean value of 153° and a much larger rms deviation of ~6%. The mean value of the O—Si—O tetrahedral angle is 109.3° and, again, a larger rms deviation of ~6%. The density for this model was found to be 1.99 g/cm$^3$, about 10% less than the experimentally measured value of 2.2 g/cm$^3$ for $a$-$SiO_2$.[42] The radial distribution function (RDF), however, shows peaks at approximately the same Si-O, O-O, and Si-Si distances as found in $\alpha$-quartz and as found experimentally[43] for $a$-$SiO_2$. We calculated the densities of states for five tetrahedra which were representative of the entire cluster. The Si—O bond-length distribution for these tetrahedra is the same as for the entire cluster. It is almost symmetric around the mean value of 1.6 Å, with a maximum deviation of ~10% in the bond length. The DOS for the $a$-$SiO_2$ (BD) are then obtained from an average value of the DOS at Si and O sites for these tetrahedra.

The second model for $a$-$SiO_2$ used in this calculation which will be henceforth referred to as $a$-$SiO_2$ (MD), was obtained by Doan[44] from a molecular-dynamics calculation. The starting point for this calculation was the $\beta$-cristoballite lattice with the density of $a$-$SiO_2$. A cubic cell with 648 atoms with periodic boundary conditions was heated to the melting point and then quenched rapidly to room temperature. The interatomic interactions were represented by Born-Mayer-Huggins[45] pair potential, which has been used previously by several authors[46–48] in simulation work on $SiO_2$. Since the procedure followed in the molecular-dynamics calculation is similar to the one used in the actual fabrication of a glass, one expects the atomic coordinates resulting from such a calculation to be better representative of the glass network. The RDF from this calculation is in good agreement with the experimental data.[43] In particular, the first three major peaks corresponding to Si-O, O-O, and Si-Si separations are correctly reproduced. Although the starting point for this calculation was the $\beta$-cristobalite lattice with a Si—O—Si bond angle of 180°, the final Si—O—Si bond angle for the amorphous state has a broad maximum at 144° and the Si—O bond length peaks at 1.62 Å. The Si—O bond-length distribution is, however, somewhat asymmetric, with one finding more Si—O longer bonds than shorter bonds. Furthermore, the maximum deviation in the bond length from its peak value is larger (~15%) than in the model of Bell and Dean. These large bond-length distortions are to be compared with rather weak distortions which are obtained by Ching[31] in his three models for $a$-$SiO_2$. There the rms deviation ranged from 0.7% to 1.7% and a maximum deviation of 3—5% of the mean bond length. The calculation of the densities of states for this model $a$-$SiO_2$ (MD) was performed in a manner similar to that described above for $a$-$SiO_2$ (BD), except that seven tetrahedra were used in the averaging procedure.

In order to keep the comparison as close as possible between $a$-$SiO_2$ and $\alpha$-quartz, a cluster of 576 atoms representing 64 unit cells was used for $\alpha$-quartz. This practically eliminates cluster-size effects in a comparative study of the electronic structures of $a$-$SiO_2$ and $\alpha$-quartz, and thus allows extraction of the effects of disorder. Thirty levels of recursions were used in all of our calculations, after which the recursion coefficients were given constant values derived from the band limits. This method of terminating the recursion coefficients amounts to embedding the cluster in an infinite solid. The high level of recursion used in this calculation ensured that the DOS was practically negligible in the band gap. A Gaussian with a half-width at half maximum (HWHM) of 0.3 eV was used to broaden the DOS in all cases, except when stated otherwise. The tight-binding parameters were taken from O'Reilly and Robertson[41] and a $1/d^2$ dependence, where $d$ is the interatomic separation, was assumed for the hopping integrals. As in earlier works,[36,41] only the nearest-neighbor Si-O and the next-nearest-neighbor O-O interactions were included, and the next-nearest-neighbor Si-Si interactions were assumed to be screened by the intervening oxygen atoms.

## III. RESULTS AND DISCUSSION

A comparison of the electronic structure of $\alpha$-quartz and $a$-$SiO_2$ can be facilitated by first discussing the effects of bond-angle—versus—bond-length disorder on different parameters. Indeed, the bond angles and bond lengths are intimately intertwined, since a change in bond angle changes the bond length and vice versa, and hence it is not possible to separate completely the effect of one from another. However, since we include only the nearest-neighbor Si-O and O-O interactions in our model, a qualitative discussion of these two effects is possible on a local level by expressing the effect of bond-angle disorders in terms of interatomic separation. Furthermore, we can assume that the Si—O bond lengths and Si—O—Si and O—Si—O bond angles are the controlling factors and Si-Si and O-O distances are determined by them. Then it is easy to show that for a given set of Si—O bond lengths, the fluctuations in the Si—O—Si bond angle has the minimum effect on the electronic structure. Such a fluctuation only changes the Si-Si distance, and since Si-Si interactions are not included in our calculation, the net effect is indirect through distant-neighbor interactions. This is not so for the fluctuations in the tetrahedral O—Si—O angle, which is a determining factor in the O-O separations. Thus for a given set of Si—O bond lengths, one can show that a change in the tetrahedral angle of 5° (which is ~5% of the ideal tetrahedral angle) causes a change of ~3% in the O-O separation. This is the same change which will be obtained if one keeps the tetrahedral angle at its ideal value but changes one of the bond lengths by ~5%. Thus the fluctuations in Si—O bond lengths will affect mostly all those states which result from either Si-O or O-O interactions or both, while the fluctuations in the tetrahedral angle will affect mostly the states governed predominantly by O-O interactions. Assuming fluctuations in tetrahedral angle to be small, we expect the Si—O bond-length fluctuations to be the governing factor in determining the electronic structure of $a$-$SiO_2$. We should emphasize that the discussion given above is quite approximate and all along it has been as-

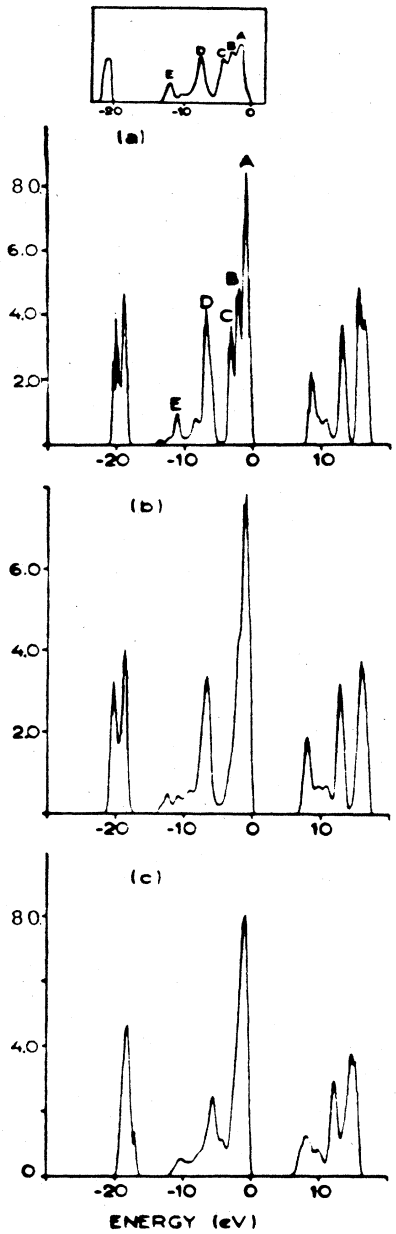


FIG. 1. Densities of states (DOS) of $SiO_2$ of two spins (in states/eV molecule) as a function of energy for (a) $\alpha$-quartz, (b) $a$-$SiO_2$ (BD), and (c) $a$-$SiO_2$ (MD). For comparison, the DOS (in arbitrary units) calculated by Chelikowsky and Schlüter for $\alpha$-quartz is shown at the top inset. Note that the energy scale matches with the rest of the figure.

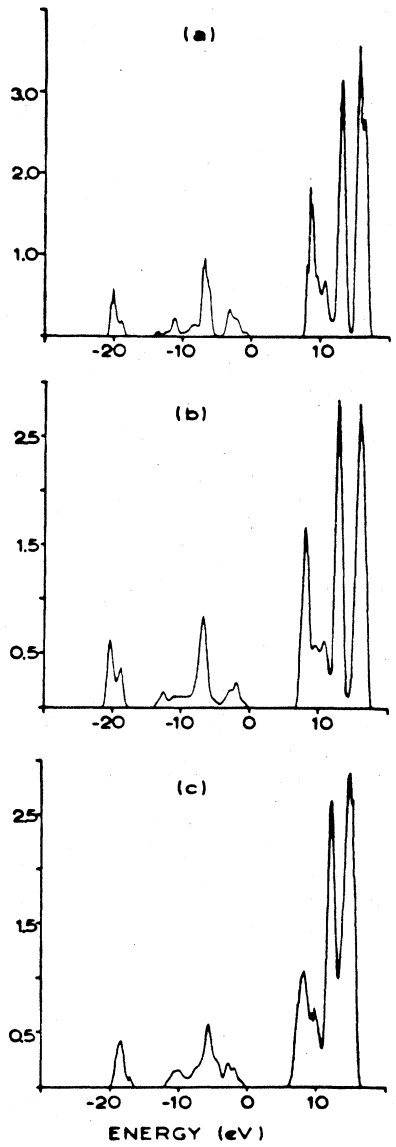


FIG. 2. DOS at the Si site (in states/eV atom) for (a) $\alpha$-quartz, (b) $a$-$SiO_2$ (BD), and (c) $a$-$SiO_2$ (MD).

sumed that the distortions in $a$-$SiO_2$ from the bond angles and bond lengths from the values in $\alpha$-quartz are small.

In Fig. 1 we show the total densities of states for the three models of $SiO_2$, namely $\alpha$-quartz, $a$-$SiO_2$ (BD), and $a$-$SiO_2$ (MD), described in Sec. II. In order to understand the nature of the bonding and the effect of disorder on the electronic structure of $SiO_2$, we have shown in Figs. 2 and 3 the local DOS on the Si and O sites. A further decomposition of these DOS's into the angular-momentum $s$ and $p$ components is shown in Figs. 4—7. From these figures, one notices a rather striking similarity in the electronic structures of $SiO_2$ in the crystalline and amorphous forms. Some structure present in the DOS in $\alpha$-quartz has been washed out in $a$-$SiO_2$ because of disorder, but the major features have remained intact, indicating the importance of short-range order in this compound. The valence and conduction bands are separated by a wide band gap. An interesting feature in $a$-$SiO_2$ is that the valence-band edge is as sharp as in the crystalline case and remains unperturbated by disorder. The conduction-band edge is sharp in the crystalline case, as expected, but shows a small amount of band tailing in the amorphous form.

The valence band is approximately 22 eV in width and

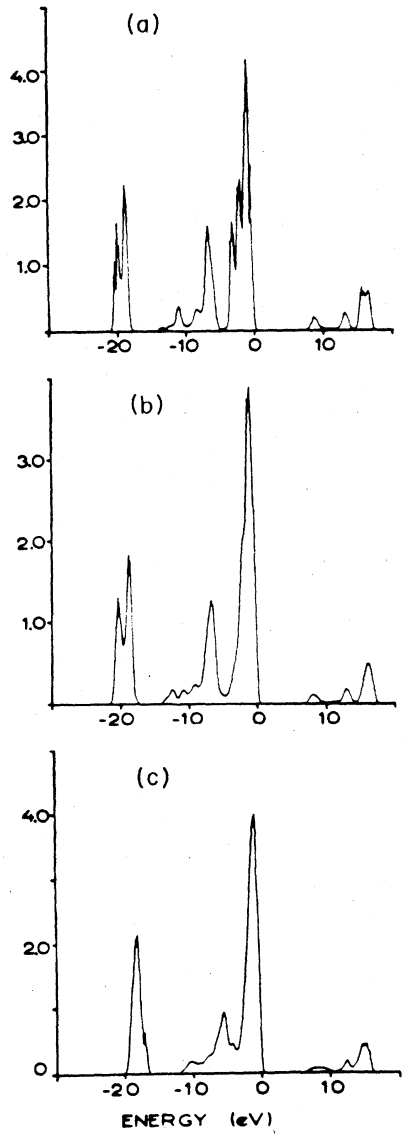


FIG. 3. DOS at the O site (in states/eV atom) for (a) $\alpha$-quartz, (b) $a$-$SiO_2$ (BD), and (c) $a$-$SiO_2$ (MD).

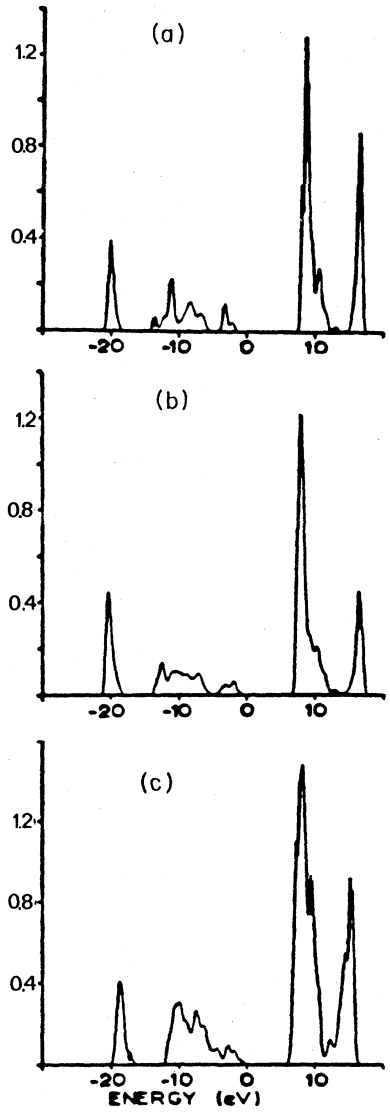


FIG. 4. The angular-momentum-decomposed partial DOS (PDOS) of $s$ type at the Si site (in states/eV atom) for (a) $\alpha$-quartz, (b) $a$-$SiO_2$ (BD), and (c) $a$-$SiO_2$ (MD).

can be separated into three distinct regions: (a) the band centered at $\sim 20$ eV; (b) states in the energy range $\sim -13$ to $-5$ eV, and (c) the top of the valence band in the energy range $-4$ to 0.0 eV. The lowest band, at $\sim -20$ eV, is predominantly of O $2s$ character, but does contain some hybridization with Si $3s$ and $3p$ states and a much smaller amount of hybridization with the O $2p$ states, as was found in earlier calculations. In the case of $\alpha$-quartz this band has a width of $\sim 2.5$ eV and shows some sharp two-peak structure. In $a$-$SiO_2$ (BD) the width is somewhat larger and the structure is reduced, but not completely wiped out. In $a$-$SiO_2$ (MD) the width is also somewhat larger, but the two-peak structure has merged to form a single peak. Furthermore, the states have shifted towards higher energies. This shows that these low-lying states, which one intuitively thinks of as core states, are affected by disorder. The reason for this can be traced to the fact that these states are formed by the next-nearest-neighbor oxygen-oxygen interactions. As mentioned in Sec. II, each oxygen atom has six oxygen-atom neighbors. In $\alpha$-quartz three of these oxygen atoms lie approximately at a distance of 2.60 Å and the other three at a distance of 2.67 Å. This small difference of $\sim 3\%$ in the oxygen-oxygen separation results in a two-peak structure since one-half of the oxygen atoms experience a stronger interaction than the other half. In $a$-$SiO_2$ (BD) there is some small dispersion, $\sim 10\%$ around these values, which leads to a somewhat larger bandwidth, but preserves the two-peak structure since this dispersion is quite symmetric around the mean oxygen-oxygen separation in $\alpha$-quartz. In $a$-$SiO_2$ (MD) there is a large variation in the oxygen-oxygen distance and, furthermore, this is asym-

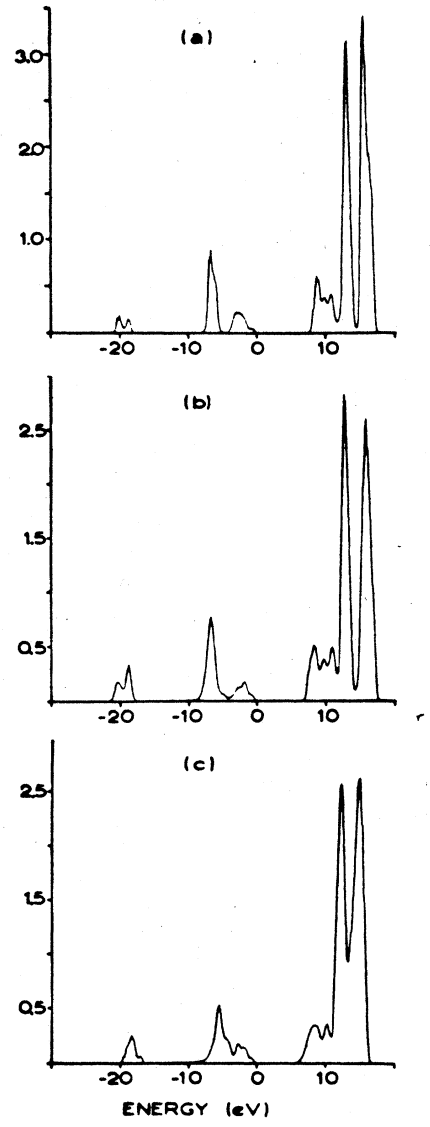


FIG. 5. PDOS of $p$ type at the Si site (in states/eV atom) for (a) $\alpha$-quartz, (b) $a$-$SiO_2$ (BD), and (c) $a$-$SiO_2$ (MD).

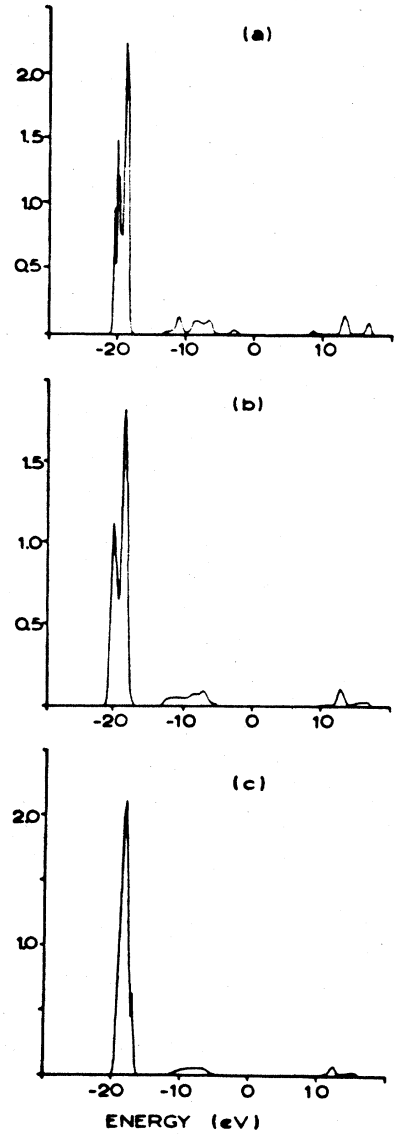


FIG. 6. PDOS of $s$ type at the O site (in states/eV atom) for (a) $\alpha$-quartz, (b) $a$-$SiO_2$ (BD), and (c) $a$-$SiO_2$ (MD).

metric, favoring more oxygen-oxygen pairs separated by longer distances. This results in the shift of the band toward higher energies, because of the weaker oxygen-oxygen interactions, and the merging of the two peaks into a single one.

The top part of the valence band from the valence-band maximum to approximately $-4$ eV is composed essentially of oxygen $2p$ states, as can be seen from Figs. 4—7. These are thus nonbonding oxygen $2p$ states with very weak interaction with nearest-neighbor silicons and their dispersion results primarily from the next-nearest-neighbor oxygen-oxygen interactions. In the case of $\alpha$-quartz we obtain a sharp three-peak structure similar to that obtained by Chelikowsky and Schlüter (we have labeled them $A$, $B$, and $C$ following their notation). From an analysis of the partial DOS shown in Figs. 4—7, we find that the uppermost peak—labeled $A$—has the weakest hybridization with the Si orbitals, and is thus of a more nonbonding nature than the lower two peaks, $B$ and $C$. These states therefore result from O $2p$ orbitals pointing in a direction perpendicular to the Si-O-Si plane. If the Si—O—Si angle was 180°, there would be another nonbonding orbital which would be pointing perpendicular to the Si-O-Si axis. In $\alpha$-quartz the angle is, however, 144°, which allows some mixing with the Si orbitals. The states associated with peaks $B$ and $C$ are derived from such nonbonding orbitals. This interpretation, based on our partial DOS analysis, is in agreement with the conclusions drawn by Chelikowsky and Schlüter on the basis of an analysis of their charge densities. The effect of structural disorder is essentially to bring two changes in the nonbonding portion of the DOS, as can be seen from

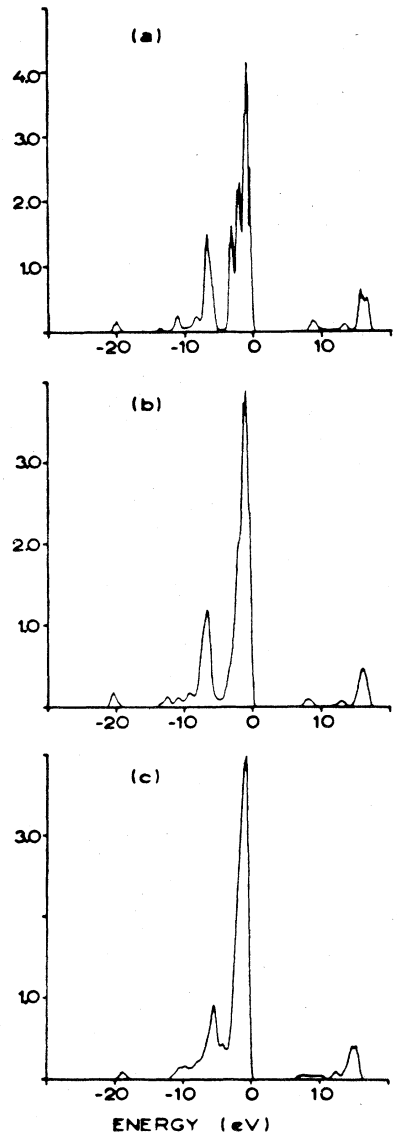


FIG. 7. PDOS of $p$ type at the O site (in states/eV atom) for (a) $\alpha$-quartz, (b) $a$-$SiO_2$ (BD), and (c) $a$-$SiO_2$ (MD).

Figs. 1—7; first, the three-peak structure found in $\alpha$-quartz is washed out, and, second, the vanishingly small DOS in the valley at $\sim -4$ eV in $\alpha$-quartz is replaced by a valley where the DOS is still low but nevertheless quite substantial. In the model of Bell and Dean the bond-length distortions from the structure in $\alpha$-quartz are small, which is why the DOS in the valley in $a$-$SiO_2$ (BD) is much smaller (see Fig. 1) than in $a$-$SiO_2$ (MD), where the bond-length distortions are much larger as was stated previously. However, the disappearance of the three-peak structure in $a$-$SiO_2$ (BD) indicates that this structure in $\alpha$-quartz is quite likely related to the Van Hove—type singularities in the band structure reflecting the effect of long-range order. The asymmetry in the bond-length distribution in $a$-$SiO_2$ (MD) favoring longer Si—O bond lengths not only affects the low-lying O $2s$ states but also the nonbonding O $2p$ states. As can be seen from Fig. 1, these nonbonding states have a smaller width, $\sim 0.35$ eV, in $a$-$SiO_2$ (MD) than that $\sim 4$ eV in $\alpha$-quartz and $a$-$SiO_2$ (BD), because of the weaker oxygen-oxygen interactions resulting from larger oxygen-oxygen separations. This width of nonbonding states is in agreement with the experimental width of $\sim 3.2$ eV on $a$-$SiO_2$.[7]

It can be seen from Figs. 2 and 3 that the states resulting from the bonding between Si and O orbitals are contained essentially in the energy range $\sim -13$ eV to $-5$ eV for $\alpha$-quartz and $a$-$SiO_2$ (BD) and in the range $\sim 11.5$ to $-5$ eV for $a$-$SiO_2$ (MD). The width of the bonding band is thus somewhat smaller in $a$-$SiO_2$ (MD) than in $a$-$SiO_2$ (BD) and in $\alpha$-quartz, again reflecting a bond-length distribution favoring longer Si—O bonds in the former case. The bandwidths for the bonding states obtained in the present work are in agreement with the experimental results on $a$-$SiO_2$.[7] We see from Fig. 1 that one interesting effect of disorder on the bonding states in $SiO_2$ is to reduce peak $D$ and wipe out peak $E$, and to fill up the shallow region in between these two peaks obtained in $\alpha$-quartz. It should be noted from Figs. 4—7 that although the valence band is dominated by the oxygen states (indeed, only $\sim 10\%$ of the total charge in the valence band in $SiO_2$ is located at the Si site), it should not be construed to mean a weak bonding. The large oxygen DOS simply reflects the fact that there are 12 electrons of oxygen participating in the bonding compared to four for silicon. The DOS in the bonding band arises essentially from the O $2p$—Si $3s\,3p$ interactions, but there is a weak participation of the O $2s$ states also. From an analysis of the DOS in the valence band, we find an electronic charge of 1.68, 1.68, and 1.48 at the Si site and 7.16, 7.16, and 7.26 at the O site for $\alpha$-quartz, $a$-$SiO_2$ (BD), and $a$-$SiO_2$ (MD), respectively. These results indicate that there is some charge transfer from silicon to oxygen atoms. The net effective charge on the oxygen site is the same in $\alpha$-quartz and $a$-$SiO_2$ (BD), but is slightly larger in $a$-$SiO_2$ (MD). Roughly speaking, we can assign an effective charge of 7.20 electrons at the oxygen site and 1.60 electrons at the silicon site in $SiO_2$ in its crystalline and amorphous states. These values are in agreement with those obtained by Pantelides and Harrison[26] and by Yip and Fowler.[24] In contrast, Ching[31] obtained significantly different values of approximately 0.92 and 7.54 electrons at silicon and oxygen sites, respectively, in his LCAO calculations. Our partial DOS analysis indicates total $s$ and $p$ charges of 0.58 and 0.90, respectively, at the Si site, and 1.90 and 5.36 at the O site in the valence band in $a$-$SiO_2$ (MD). A further examination shows that out of 1.90 O $2s$ electrons in the valence band, only 1.75 are located in the lowest band at $\sim -20$ eV and the rest are distributed essentially in the bonding portion of the band. Furthermore, the remaining 0.10 O $2s$ electron is to be found in the conduction band. This suggests that O $2s$ electrons do play some role in bonding in $SiO_2$ as was proposed by Laughlin *et al.*[36] The lowest "O $2s$" band derives roughly 10% of its charge mostly from the Si $3s$ and $3p$ states and some from O $2p$ states, their contributions being 0.08, 0.10, and 0.07 electron, respectively. Similar results are obtained for $\alpha$-quartz and $a$-$SiO_2$ (BD).

The antibonding states form the lowest part of the conduction band. Since O $3s$ and Si $3d$ orbitals are not included in our calculation, the conduction band presented here should be considered only approximate. The partial DOS presented in Figs. 4—7 shows that the conduction band not only contains significant O $2p$ character but also a weak O $2s$ character. We obtain three major peaks in $\alpha$-quartz which are preserved in $a$-$SiO_2$ (BD) and $a$-$SiO_2$ (MD), but with reduced strengths. The middle peak is composed of essentially Si $3p$ states, but the first and the third contain significant hybridization of the Si $3s$ states with the Si $3p$ states. The major effect of disorder is to reduce the band gap slightly. We find a band gap of 8.4, 7.5, and 7.2 eV, respectively, in $\alpha$-quartz, $a$-$SiO_2$ (BD), and $a$-$SiO_2$ (MD) with a band tailing of $\sim$0.3 eV in the amorphous case. This is to be compared with the experimental value of 8.9 eV obtained by Distefano and Eastman[15] from photoconductivity measurements in $a$-$SiO_2$. The experimental value was obtained from a quadratic fit of the absorption coefficient above the gap. A careful examination of Fig. 1 of Ref. 15 shows that the absorption sets in somewhat earlier and a lower value of $\sim$8.5—8.7 eV would be more appropriate. Our value of 8.5 eV for $\alpha$-quartz is a little bit lower than the value of 9.2 eV obtained by Chelikowsky and Schlüter[30] but is in agreement with the value of 8.4 eV obtained by Ching.[31] Ching also found that the effect of disorder was to reduce the band gap, but he obtained much smaller values. For one of the models he constructed he obtained a band gap as low as 6.17 eV, but the average value for all of his three models was $\sim$7.2 eV. The decrease in the band gap due to disorder has also been found in the elemental semiconductors.[49—50] A similar trend has been found experimentally[9] for $SiO_2$.

## IV. COMPARISON WITH EXPERIMENTAL DATA

We now turn to a comparison of our results with the experimental data obtained using several optical techniques. The latter are powerful techniques to probe the electronic structure of insulators. The x-ray emission, XPS, UPS, and optical reflectivity all probe features of the electronic structure which are not always the same and are sometimes complimentary.

### A. X-ray emission

In x-ray emission an electron from the valence band drops into an empty core state, emitting a photon in the process. The vacancies in the core levels are created by bombarding the sample with energetic electrons or x-rays. Although the energy of the bombarding electron beam is low ($\sim$3 keV for the Si $K$ spectrum) to rule out defect production by displacement, atomic displacements can still occur in some insulators by the mechanism of radiolysis[51] involving electron-hole recombination. This can sometimes complicate the interpretation of some x-ray-emission spectra. We leave this point for the moment and return to it later. The transition probability of an electron from the valence band combining with an empty core level is governed by the dipole-selection rules. If the core levels are localized and the overlap with the neighboring atomic states can be neglected, then the emission spectrum yields direct information about the composition of DOS's locally at the probe site. Thus Si $K$ emission is derived from the Si $p$ DOS in the valence band, while the Si $L_{2,3}$ emission is derived from a mixture of both Si $s$—type and Si $d$—type DOS. Similarly, O $K$ emission depends upon the O $p$—type DOS. It can be shown quite generally that the shape $I(E)$ of a silicon $L_{2,3}$ spectrum at energy $E$, for example, is given by, apart from a multiplicative factor,

$$I(E)=N_s(E)f_s(E)+N_d(E)f_d(E)\ , \tag{1}$$

where $N_s$ and $N_d$ are the partial $s$- and $d$-type DOS's at the Si site, and $f_s$ and $f_d$ are functions which result from the dipole matrix elements and, generally speaking, are smoothly and slowly varying functions of the energy $E$. Thus the structure in the emission spectrum can be directly correlated with the structure in the DOS, except for its height.[52]

All three possible emission spectra in $\alpha$-quartz, namely Si $K$ and $L_{2,3}$ and O $K$, have been measured,[3—6] and the Si $K$-emission spectrum has also been measured[3] for $a$-$SiO_2$. We present in Figs. 8—10 these spectra, along with our relevant partial DOS (PDOS), which have been broadened by a Gaussian with a HWHM of 0.7 eV (this is to be compared with 0.3 eV used in Figs. 1—7) to reflect the broadening resulting from core-hole lifetime effects and instrumental resolution. The theoretical Si $S_{2,3}$ spectrum contains only the partial $s$ DOS at the Si site since no $d$ orbitals are included in our calculation.

Since the valence-band DOS is dominated by the oxygen $2p$ states, it is interesting to first look at the O $K$ emission, which samples the O $p$ states. The experimental spectrum (for $\alpha$-quartz) shows a sharp maximum and a shoulder with a small maximum, the two maxima being separated by $\sim$5 eV (see Fig. 8). These features are reproduced in our calculation for all three models. Our calculations, however, also suggest some differences between $\alpha$-quartz and $a$-$SiO_2$ and it will be interesting to measure this spectrum for $\alpha$-$SiO_2$. For $\alpha$-quartz we find a major peak at $-1.3$ eV in the nonbonding region, and a smaller peak at $-6.5$ eV and a small peak at $-10.9$ eV in the bonding part of the valence band. The separation of 5.2 eV between the first two peaks is in agreement with the experimental value in $\alpha$-quartz. In $a$-$SiO_2$ (BD) similar features are obtained, except that the separation between the two peaks is slightly larger ($\sim$5.6 eV) and the much weaker third peak is washed out by disorder. Our third model for $SiO_2$, namely $a$-$SiO_2$ (MD), also yields qualitatively similar features, but, in contrast, a smaller separation of 4.4 eV is obtained. In view of the fact that this latter model yields a valence-band width of 11.5 eV (not counting the O $2s$ states), which is in good agreement with the experimentally determined[7] bandwidth of 11.2 eV for $a$-$SiO_2$, we expect the separation between the two peaks in the O $K$ spectrum to become narrower in going from $\alpha$-quartz to $a$-$SiO_2$ and it will be interesting to verify this point experimentally. On the basis of our calculations, the first peak can be assigned to the completely nonbonding O $2p$ states and the second peak to the O $2p$

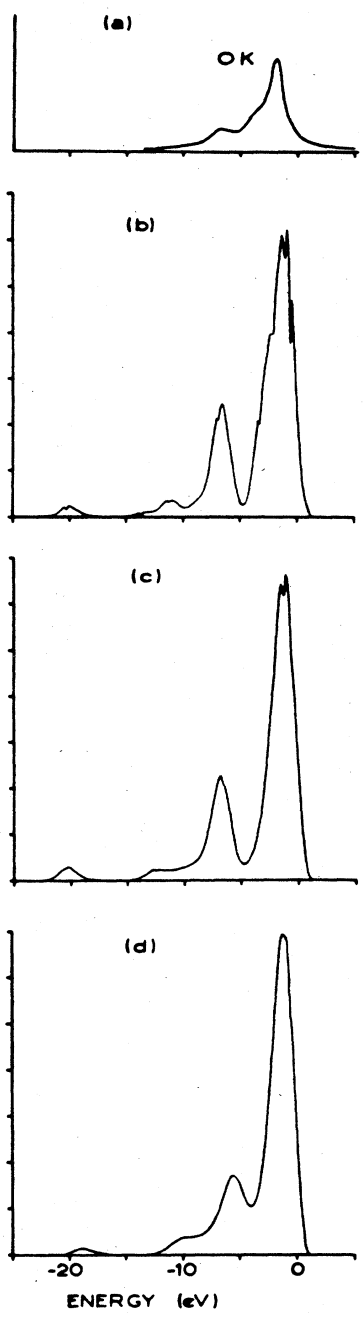


FIG. 8. O $K$ x-ray-emission spectrum of $SiO_2$; (a) experimental curve from Ref. 3 for $\alpha$-quartz, and calculated curves for (b) $\alpha$-quartz, (c) $a$-$SiO_2$ (BD), and (d) $a$-$SiO_2$ (MD).

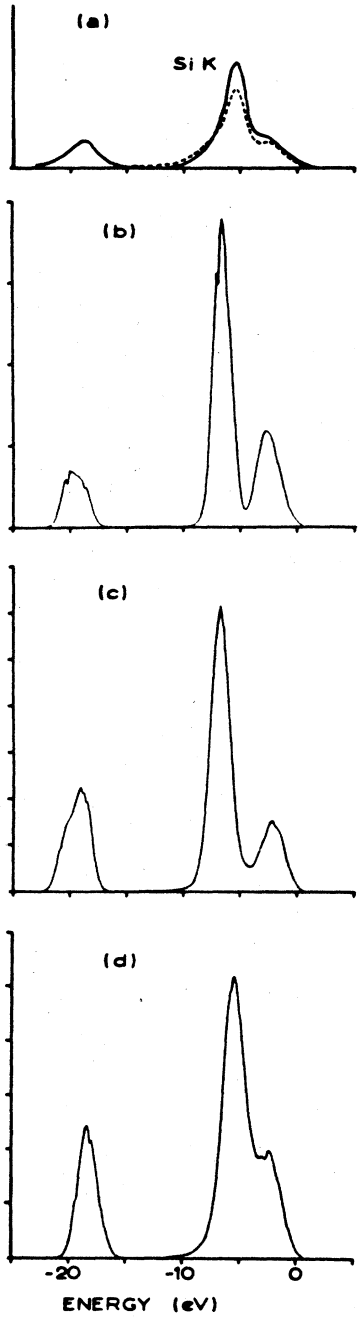


FIG. 9. Si $K$ x-ray-emission spectrum for $SiO_2$; (a) experimental curves (from Ref. 3), $\alpha$-quartz (solid line), $a$-$SiO_2$ (dotted line), and calculated curves for (b) $\alpha$-quartz, (c) $a$-$SiO_2$ (BD), and (d) $a$-$SiO_2$ (MD).

bonding states. Apart from this, we find a small O $2p$ admixture also with the O $2s$ states, which has not been observed experimentally and is probably suppressed by the matrix elements.

The experimental Si $K$ spectrum[3] also displays a sharp peak and a small peak or a shoulder (closer to the valence-band maximum) which are separated by $\sim 2.3$ eV in $\alpha$-quartz and $\sim 3.0$ eV in $a$-$SiO_2$ (see Fig. 9). There is some emission also seen from the lowest part of the valence band situated at $\sim -20$ eV. Again these features are reproduced in our calculation. For $\alpha$-quartz we find a small peak at $-2.6$ eV and a large peak at $-6.5$ eV. This, however, gives a separation of 3.9 eV, which is larger than the experimental value. In the model of Bell and Dean, namely $a$-$SiO_2$ (BD), these features are retained, except the peak positions are somewhat shifted

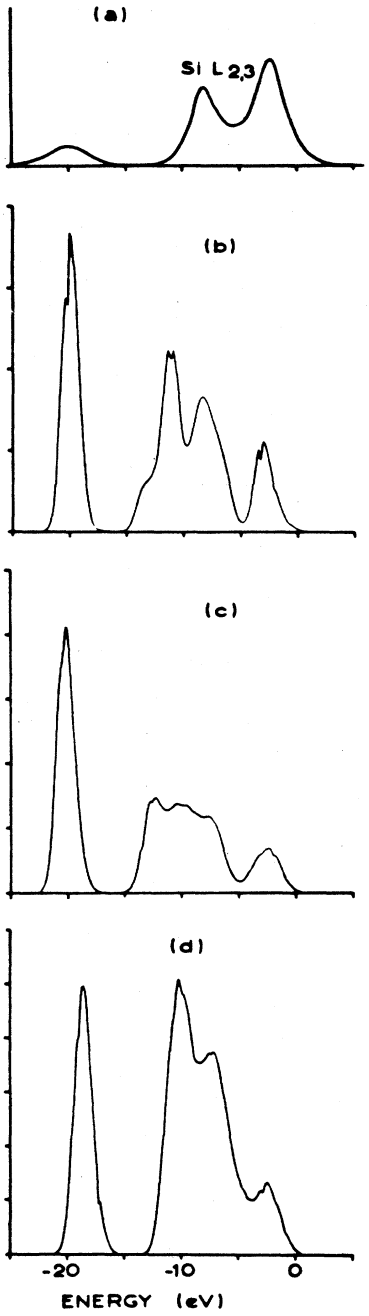


FIG. 10. Si $L_{2,3}$ x-ray-emission spectrum for $SiO_2$; (a) experimental curve (from Ref. 4) for $\alpha$-quartz, and calculated curves for (b) $\alpha$-quartz, (c) $a$-$SiO_2$ (BD), and (d) $a$-$SiO_2$ (MD).

and one obtains a separation of 4.3 eV, again larger than the experimental value for $a$-$SiO_2$. Our spectrum for $a$-$SiO_2$ (MD) is, however, closer to the experimental one for $a$-$SiO_2$, where we obtain a peak at $-5.3$ eV and a shoulder at $-2.3$ eV. This gives us a separation of 3.0 eV, as observed experimentally. In all three models we also find significant emission from the lowest part of the band formed of "oxygen $2s$" states, indicating some hybridization between O $2s$ and Si $3p$ states. It should be noted that the shoulder (or the small peak) in our calculated Si $K$ spectrum arises from the second set of nonbonding oxygen states closer to the bonding silicon-oxygen states, allowing some hybridization, whereas the large peak is derived from the region of bonding states.

This is to be compared to the case of O $K$ emission, where the large peak was derived from the completely nonbonding O $2p$ states closest to the top of the valence band and the shoulder from the bonding states. Because of this difference in the two types of nonbonding states and the shift between them, the matching of the peak position of the O $K$ emission with the shoulder of the Si $K$ emission used by Klein and Chun[3] to obtain their energy scales for their spectra is not correct. We should point out that our results for these spectra are in agreement with an earlier calculation by Chelikowsky and Schlüter[30] for $\alpha$-quartz. Pantelides and Harrison[26] have also given a discussion of these spectra in terms of their bond-orbital model.

The Si $L_{2,3}$— emission spectrum is shown in Fig. 10. The experimental curve for $\alpha$-quartz shows an almost symmetric two-peak structure separated by $\sim 6$ eV (Ref. 3) in the bonding-nonbonding region. Our calculated Si $s$ PDOS for $\alpha$-quartz, on contrast, displays three peaks at $-3.0$, $-8.3$, and $-11.0$ eV, the first derived from the nonbonding region and the latter two from the bonding region. Furthermore, the height of the peak in the nonbonding region is somewhat lower than the heights of the other two peaks (actually, it is one-half the height of the peak at $-11.0$ eV). These results are qualitatively similar to those obtained by Chelikowsky and Schlüter in their pseudopotential calculation. These authors obtained a peak at $\sim -12$ eV and a shoulder at $\sim -9$ eV in the bonding region, and a broad peak at $\sim -3$ eV in the nonbonding region. The latter peak was, however, only about a fourth of the height of the peak at $-12$ eV. Fowler and co-workers[27–28] also find a rather weak $s$ character at the silicon site in the nonbonding region. To account for the experimental spectrum, where the height of the peak in the nonbonding region is somewhat higher than that of the one in the bonding region, two types of arguments have been put forward. Based on early molecular cluster calculations,[21] it has been suggested that some Si $3d$ component is present in the valence band and the peak in the nonbonding region will be enhanced if this contribution, however small, was included. More recent calculations[22] have, however, yielded no significant $d$ character in the valence band. The second proposal[30] concerns the state of the sample. It has been argued that the process of bombardment of $\alpha$-quartz by electrons before emission of x-rays creates regions rich in silicon which lead to an increased height of the peak in the nonbonding region. While electron beam does create damage in $SiO_2$,[4] this damage, however, anneals quite rapidly at the temperature at which the spectrum is recorded,[4] and thus the observed spectrum reflects the spectrum of Si in $\alpha$-quartz.

The discrepancy in the relative heights of the calculated and experimental peaks is, however, only a part of the problem. The separation between the two outermost peaks, both in the present work and in the calculation of Chelikowsky and Schlüter,[30] is also larger ($\sim$8—9 eV)

than observed experimentally ($\sim 6$ eV). We believe that the $L_{2,3}$-emission spectrum in $SiO_2$ is strongly influenced by the matrix elements,[53] and an accurate calculation of these is necessary for a proper understanding of this spectrum. We note that our $s$ PDOS at the silicon site already has the essential features. Indeed, a slowly decreasing matrix element away from the top of the valence band could quite likely merge the two peaks at $-11.1$ and $-8.3$ eV into one at around $-9.5$ eV and raise the relative height of the one at $-3.0$ eV.

The experimental $L_{2,3}$ spectrum for $\alpha$-quartz also shows some emission from the lowest portion of the valence band situated at $\sim -20$ eV. This is also found in our calculation since there is a significant Si $s$ PDOS in this band.

Our calculated $L_{2,3}$-emission spectrum for $a$-$SiO_2$ is, roughly speaking, quite similar to the one for $\alpha$-quartz. The band around $\sim -20$ eV again has a strong $s$ component at the Si site. However, the three-peak structure is substantially broadened in the bonding-nonbonding region. The shape of this structure for $a$-$SiO_2$ (BD) and $a$-$SiO_2$ (MD) are quite similar, but the latter has a width smaller by $\sim 0.8$ eV.

### B. UPS and XPS

In UPS and XPS one measures the energy distribution of electrons emitted from the sample by incident photons; the photon energies are low in UPS but much higher in XPS. The process of ejection of electrons is again governed by the dipole-selection rules. The observed spectra therefore do not measure the true total DOS in a solid but rather a DOS weighted by different optical matrix elements. Assuming the final electron states to be nearly-free-electron-like, one finds that UPS picks out predominantly the $p$ component of the DOS while XPS strongly emphasizes the $s$ component. Since our valence-band DOS is strongly dominated by the oxygen $p$ states, UPS is the easiest to relate to our PDOS. In Fig. 11 we show the experimental UPS spectrum[7] for $a$-$SiO_2$ taken for the photon energy $\hbar\omega = 40.8$ eV. The experimental spectrum shows a peak at $-2.4$ eV in the nonbonding region and a peak at $\sim -7$ eV in the bonding region. The two peaks are separated by a shallow dip at $\sim -5$ eV. The total width of the bonding-nonbonding valence band is 11.2 eV. These features are fully reproduced in the UPS spectrum of our $a$-$SiO_2$ (MD) model shown in Fig. 11. On the other hand, the calculated UPS spectra (the $p$ PDOS of $SiO_2$) for $\alpha$-quartz and $a$-$SiO_2$ (BD) are quite similar to each other and show small qualitative differences with the calculated spectrum for $a$-$SiO_2$ (MD) and the experimental spectrum for $a$-$SiO_2$. For example, the bandwidth in both models is larger ($\sim 13$ eV) and the dip at $-5$ eV much stronger. The good agreement between the $a$-$SiO_2$ (MD) UPS spectrum and the experimental spectrum for $a$-$SiO_2$ indicates that the amorphous structure for $SiO_2$ obtained from the molecular-dynamics calculation is a good representation for $a$-$SiO_2$. This comparison also shows that the bonds in $a$-$SiO_2$ (BD) are quite strained and that there are some small yet measurable differences in the UPS spectra of $\alpha$-quartz and $a$-$SiO_2$.

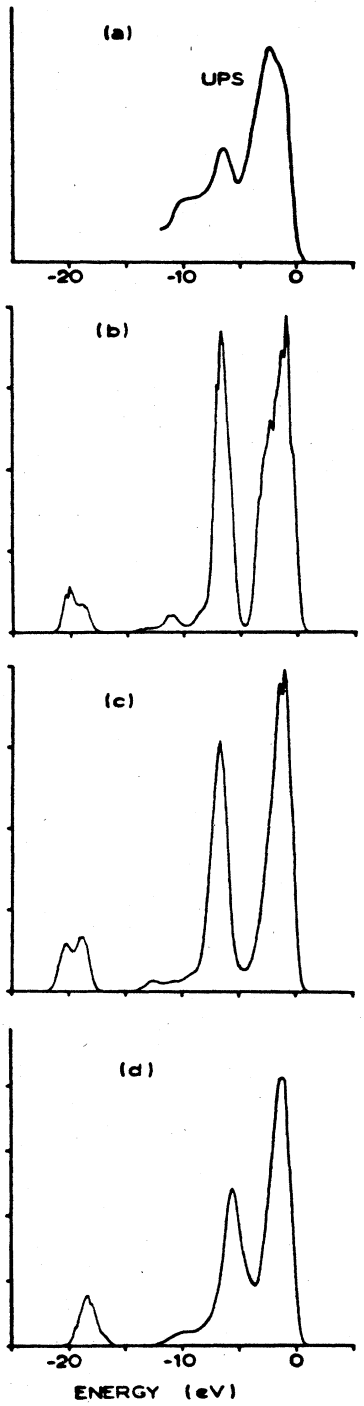


FIG. 11. UPS spectrum for $SiO_2$; (a) experimental spectrum for $a$-$SiO_2$ (from Ref. 7), and calculated curves for (b) $\alpha$-quartz, (c) $a$-$SiO_2$ (BD), and (d) $a$-$SiO_2$ (MD).

The experimental XPS spectrum[7] for $a$-$SiO_2$ for the photon energy $\hbar\omega = 1486.6$ eV is shown in Fig. 12. This spectrum, in principle, picks out strongly the states of $s$ character in the valence band due to the dipole-selection rules. In the present case of $SiO_2$ we are, however, con-

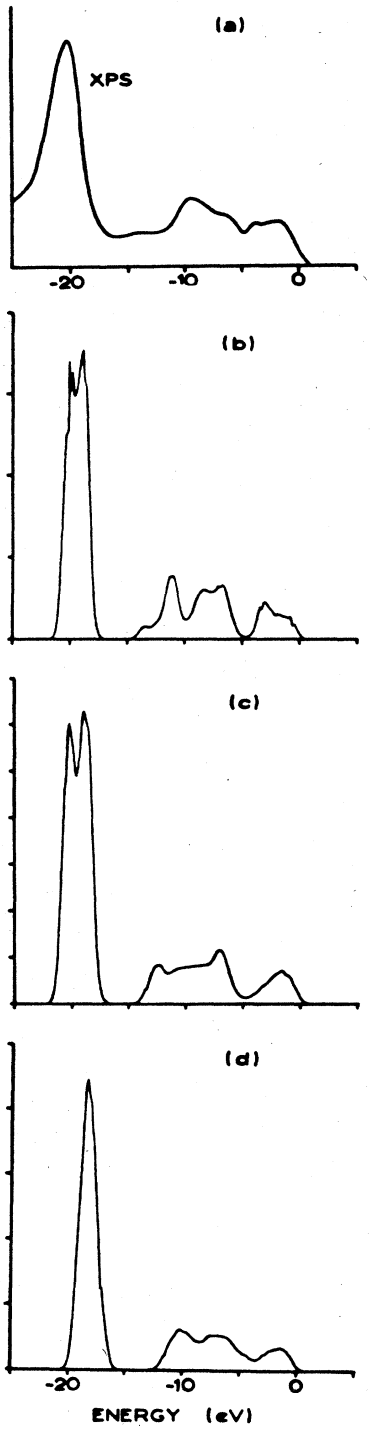


FIG. 12. XPS spectrum for $SiO_2$; (a) experimental spectrum for $a$-$SiO_2$ (from Ref. 7), and calculated curves for (b) $\alpha$-quartz, (c) $a$-$SiO_2$ (BD), and (d) $a$-$SiO_2$ (MD).

fronted with a situation where the $s$-type PDOS in the valence band is rather weak and the valence band is dominated by essentially $p$-type PDOS. Thus the inclusion of even a very small fraction of the $p$-type PDOS with the $s$ PDOS will substantially affect the calculated XPS spectrum. Further complication is added by the fact that the ratio in which the Si and O $s$ components mix is not known. Nevertheless, it is still interesting to identify the origin of the major features in the XPS spectrum by choosing ratios which will roughly reproduce the experimental spectrum. An examination of our PDOS shows that this can be done by combining the $s$-type PDOS of Si and O in equal ratios with a 3% mixture of $p$ PDOS (note that the Si $p$ component is everywhere much smaller than O $p$ component). The results are shown in Fig. 12. With this prescription we find that more than half the structure in the nonbonding region at $\sim -2$ eV can be attributed to the O $p$ states and the rest to the Si and O $s$ states. In contrast, the structure in the bonding region arises largely from the Si and O $s$ states. For example, the structure around $-10$ eV can be attributed solely to the Si $s$ states, while the one around $-7$ eV to a 2:1 contribution from the Si and O $s$ states. This analysis is in agreement with the assignment made by Fischer *et al.*[8] on the basis of molecular cluster calculations. A comparison of the experimental spectrum with the calculated spectra in the bonding-nonbonding region shows that the $a$-$SiO_2$ (MD) correctly reproduces all the major features of the experimental spectrum, including the width of the bonding-nonbonding region. The calculated spectrum for $\alpha$-quartz shows sharp features as expected, which are broadened in the $a$-$SiO_2$ (MD). The spectrum for $a$-$SiO_2$ (BD), in contrast, does retain sharp features not found in the experimental spectrum. Note that the experimental spectrum shows a large intensity from the "O 2$s$" states which is reproduced in our calculated spectra.

### C. Optical reflectivity

Phillip[16] has measured the ultraviolet optical reflectivity for $\alpha$-quartz and $a$-$SiO_2$. From these measurements he extracted the imaginary part of the dielectric function $\epsilon_2(\omega)$ for photons energy $\hbar\omega$. The spectrum for $a$-$SiO_2$ is very similar to that for $\alpha$-quartz. The spectra show peaks at 10.4, 11.7, 14.0, and 17.3 eV. The peaks are broadened in $a$-$SiO_2$, but their positions remain essentially unchanged. The imaginary part of the dielectric function is given by

$$\epsilon_2(\omega) \sim \frac{1}{\omega^2} \sum_{c,v} |M_{cv}|^2 \delta(E_c - E_v - \hbar\omega) , \tag{2}$$

where $v$ and $c$ stand for valence and conduction bands, respectively, and $E$ is the electron energy. $M_{cv}$ is the dipole matrix element for transition from the valence band to the conduction band. If $M_{cv}$ is taken to be constant, then $\epsilon_2(\omega)$ amounts to the joint densities of states. In Fig. 13 we have shown the JDOS for $\alpha$-quartz. We obtain three sharp peaks at 9.7, 14.1, and 16.4 eV. This is to be compared to the calculation of Chelikowsky and Schlüter[30] who obtained no structure below $\sim 15.3$ eV. We have not shown the JDOS for the $a$-$SiO_2$, but similar structures are obtained except that the peaks are slightly shifted in energy and broadened. As was noted by Chelikowsky and Schlüter, the JDOS is not, however, a correct representation for $\epsilon_2(\omega)$ even if matrix elements are as-

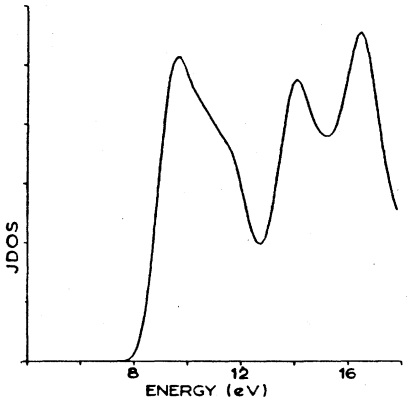


FIG. 13. JDOS for $\alpha$-quartz (in arbitrary units).

sumed constant or slowly varying. The dipole-selection rule couples states of only certain symmetry. In the present case couplings will be allowed only between $s$ and $p$ states, but not between states of the same angular momentum. Thus a better representation for $\epsilon_2(\omega)$ can be obtained by assuming the transitions to be purely intra-atomic and conserving only those permitted by the dipole-selection rules. Furthermore, the crystal-momentum-conservation rule can be ignored in the case of $a$-$SiO_2$ and we can adopt the indirect constant matrix-element approximation.[54] We follow the same procedure for $\alpha$-quartz to keep the comparison as close as possible with $a$-$SiO_2$ (note that in our method $\alpha$-quartz and $a$-$SiO_2$ are treated on the same footing and nowhere do we take advantage of periodicity). In Figs. 14 and 15 we have shown contributions from Si and O sites respectively to $\epsilon_2(\omega)$ for $\alpha$-quartz, $a$-$SiO_2$ (BD), and $a$-$SiO_2$ (MD). We have found that the transition from the $p$ states in the valence band play the dominating role at both silicon and oxygen sites. The curves at the oxygen site are strikingly similar for $\alpha$-quartz and $a$-$SiO_2$. For $\alpha$-quartz we obtain two peaks, at 9.5 and 14.0 eV. The same two peaks are also found for $a$-$SiO_2$ (BD) and $a$-$SiO_2$ (MD), except that the peaks are slightly shifted towards lower energies to reflect the reduced band gap. Two peaks are also obtained from the Si site, but the detailed structure in this case does depend on the underlying structural model. For example, the second peak shifts from 15.2 eV in $\alpha$-quartz to 13.6 eV in $a$-$SiO_2$ (MD). The position of the first peak depends on the band gap essentially. It is found at 11.2 eV in $\alpha$-quartz and around $\sim 10.2$ eV in $a$-$SiO_2$ (BD) and $a$-$SiO_2$ (MD). It should be emphasized that our conduction band is quite approximate and so our peak positions are only qualitative. Furthermore, a full account of the matrix elements has not been taken. Nevertheless, these calculations do indicate the origin of the structure observed experimentally. If our calculated peak positions were referred to a constant band gap of 9 eV in both $\alpha$-quartz and $a$-$SiO_2$, we would obtain the first three peaks at approximately 10, 11.5, and 14.5 eV in $\alpha$-quartz, and in $a$-$SiO_2$ (BD) and $a$-$SiO_2$ (MD). Considering the approximate nature of this calculation, the agreement with the experiment can be considered satisfactory. On the basis of this comparison, the first and the third peaks in the exper-

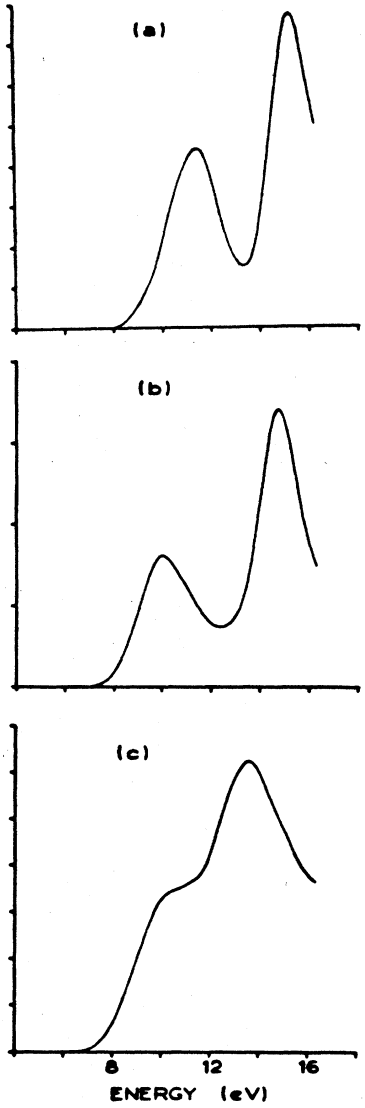


FIG. 14. Contribution from the Si site to the imaginary part of the dielectric function $\epsilon_2(\omega)$ in (a) $\alpha$-quartz, (b) $a$-$SiO_2$ (BD), and (c) $a$-$SiO_2$ (MD).

imental spectrum can be attributed to transitions from the O $2p$ states in the valence band to the O $2s$ states in the conduction band and the second peak to transitions from the Si $3p$ to Si $3s$ states. Considering the sharpness of the first peak, we believe that it is exciton-enhanced. It is noteworthy that although the three models used in our calculation are structurally quite different, they yield similar structures in $\epsilon_2(\omega)$, which is probably related to the fact that these structures originate largely from the nonbonding part of the valence band, thus reflecting the largely atomic nature of these states. The other peak associated with Si sites is not observed experimentally and is probably suppressed by matrix elements. This comparison between experiment and our calculations also suggests that the band gaps in $\alpha$-quartz and $a$-$SiO_2$ are about the same although theoretically we and other workers[31,36] find a smaller gap in the amorphous phase. The reason for this discrepancy is not clear.

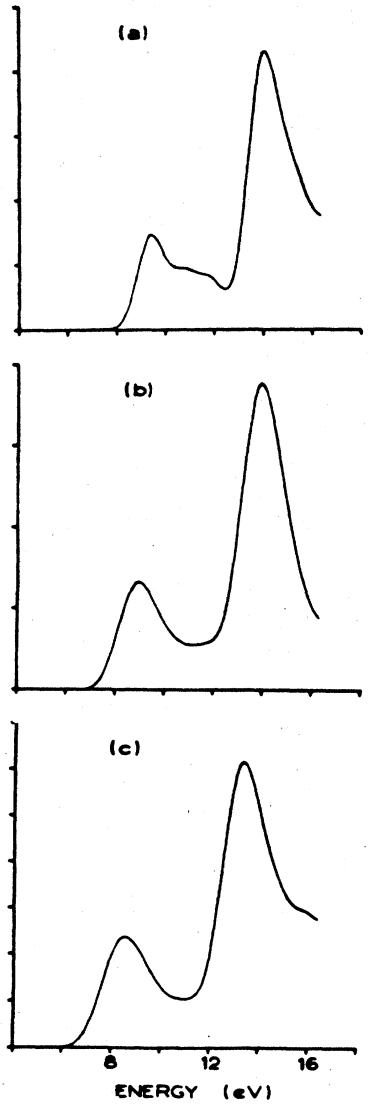


FIG. 15. Contribution to $\epsilon_2(\omega)$ from the O site in (a) $\alpha$-quartz, (b) $a$-$SiO_2$ (BD), and (c) $a$-$SiO_2$ (MD).

## V. CONCLUSION

In this paper we have attempted to investigate the effects of disorder on the electronic structure of $SiO_2$. For this purpose two different models of disorder were chosen, namely the continuous-random-network model of Bell and Dean and a model constructed from molecular-dynamics simulation. The electronic structure of $\alpha$-quartz and $a$-$SiO_2$ are on the whole quite similar, but there are differences in details. The valence band can be divided into three main regions; the lowest band at $\sim -20$ eV dominated by the O $2s$ states, the silicon-oxygen bonding band between $\sim -5$ to $-13$ eV, and the nonbonding oxygen states from the top of the valence band at 0 to $\sim -4$ eV. The band at $\sim -20$ eV is not narrow and has a width of $\sim 2.5$ eV and has unexpectedly large mixing with other orbitals. We find that roughly 1.75 electrons in this band can be associated with the O $2s$ states. The rest, 0.25 electrons, have to be attributed to the O $2p$ states (0.07 electron) and Si $s$ and $p$ states (0.08 and 0.10 electron, respectively). This hybridization is confirmed by the x-ray-emission experiments. Our calculations indicate that O $2s$ states also take part in the bonding although this is very weak. Roughly, 1.90 O $2s$ electrons are found in the valence band and 0.10 electron is spread out in the conduction band. Thus our results support the picture of bonding put forward by Laughlin *et al.*[36] We find effective charges of 7.2 and 1.6 electrons at the O and Si sites, respectively.

There are two principal changes brought about by disorder. First, the sharp structure in the valence band is smoothed out. The deep valley in the DOS between nonbonding and bonding states is replaced by a valley which is much shallower. The top of the valence band, however, remains unmoved by disorder reflecting its more atomic character. The valence-band edge thus remains sharp. This is to be contrasted with the elemental amorphous semiconductors where a small valence-band tailing is found. Second, the band gap is reduced in $a$-$SiO_2$ compared to $\alpha$-quartz. This arises by a lowering of the conduction-band edge. This trend has been found in previous calculations[31] and also in elemental semiconductors.[50,51] The reduction of the band gap has also been observed experimentally for $SiO_2$.[9] The width of the bonding-nonbonding portion of the valence band is also affected by disorder, but depends on the model. This width is found to be $\sim 13$ eV in $\alpha$-quartz. It remains practically unchanged in $a$-$SiO_2$ (BD), but is reduced to 11.5 eV in $a$-$SiO_2$ (MD). We find that, generally speaking, the results for $a$-$SiO_2$ (BD) are quite similar to those for $\alpha$-quartz. Since the bond distortions are quite small in $a$-$SiO_2$ (BD) this indicates that the local tetrahedral structure plays an essential role in determining the electronic structure of $SiO_2$. Our results for $\alpha$-quartz are in good agreement with O $K$ and Si $K$ x-ray-emission data, but for Si $L_{2,3}$ emission the agreement is only qualitative. This we attribute to the effect of matrix elements not included in our calculation. Among the two structural models which were chosen for $a$-$SiO_2$, we find that the $a$-$SiO_2$ (MD) yields results in better agreement with the experimental data (UPS, XPS) than does the $a$-$SiO_2$ (BD). This indicates that the bond distortions in $a$-$SiO_2$ are quite substantial. Finally, our calculation has also allowed us to find the origin of the peaks in the optical reflectivity spectra. We believe that the first and third peaks in the reflectivity spectrum can be attributed to transitions from the nonbonding oxygen states and the second peak to silicon states.

## ACKNOWLEDGMENTS

I would like to thank Dr. Y. Adda for his constant interest in this work and advice. I would also like to thank Dr. M. Gerl and Dr. B. Legrand for helpful discussions and N. V. Doan for providing me the atomic coordinates of his molecular-dynamics simulations.

[1]R. W. G. Wyckoff, *Crystal Structures* (Interscience, New York, 1965), Vol. 1, p. 312.
[2]D. L. Griscom, Phys. Rev. B **22**, 4192 (1980).
[3]G. Klein and H. U. Chun, Phys. Status Solidi B **49**, (1972); G. Wiech, E. Zopf, H. U. Chun, and R. Bruckner, J. Non-Cryst. Solids **21**, 251 (1976).
[4]G. Wiech, Solid State Commun. **52**, 807 (1984).
[5]D. W. Fischer, in *Advanced in X-Ray Analysis,* edited by B. L. Henke, J. B. Newkirk, and G. R. Mallet (Plenum, New York, 1970), Vol. 13, p. 182; J. Chem. Phys. **42**, 3814 (1965).
[6]O. A. Ershov, D. A. Goganov, and A. P. Lukinskii, Fiz. Tverd. Tela **7**, 2355 (1965) [Sov. Phys.—Solid State **7**, 1903 (1966)]; (1966)]; A. A. Zhdanov, *ibid.* **8**, 2137 (1966) [**8**, 1699 (1967)].
T. H. Distefano and D. E. Eastman, Phys. Rev. Lett. **27**, 1560 (1971).
[8]B. Fischer, R. A. Pollak, T. H. Distefano, and W. D. Grobman, Phys. Rev. B **15**, 3193 (1977).
[9]T. A. Stephenson and N. J. Binkowski, J. Non-Cryst. Solids **22**, 399 (1976).
[10]S. R. Nagel, J. Tauc, and B. G. Bagley, Solid State Commun. **20**, 245 (1976).
[11]J. E. Rowe, Appl. Phys. Lett. **25**, 576 (1974).
[12]H. Ibach and J. E. Rowe, Phys. Rev. B **10**, 710 (1974).
[13]R. Williams, Phys. Rev. **140**, A569 (1965).
[14]A. Koma and R. Ludeke, Phys. Rev. Lett. **35**, 107 (1975).
[15]T. H. Distefano and D. E. Eastman, Solid State Commun. **9**, 2259 (1971).
[16]H. R. Phillip, Solid State Commun. **4**, 73 (1966); J. Phys. Chem. Solids **32**, 1935 (1971).
[17]K. Platzöder, Phys. Status Solidi **29**, K63 (1968).
[18]A. R. Ruffa, Phys. Status Solidi **29**, 605 (1968); J. Non-Cryst. Solids **13**, 37 (1973/74).
[19]M. H. Reilly, J. Phys. Chem. Solids **31**, 1041 (1970).
[20]A. J. Bennett and L. M. Roth, J. Phys. Chem. Solids **32**, 1251 (1971); Phys. Rev. B **4**, 2686 (1971).
[21]G. A. D. Collins, D. W. J. Cruickshank, and A. Breeze, J. Chem. Soc. Faraday Tran. II **68**, 1189 (1972).
[22]T. L. Gilbert, W. J. Stevens, H. Schrenk, M. Yoshimine, and P. S. Bagus, Phys. Rev. B **8**, 5988 (1973).
[23]T. A. Tossell, D. J. Vaughan, and K. H. Johnson, Chem. Phys. Lett. **20**, 329 (1973).
[24]K. L. Yip and W. B. Fowler, Phys. Rev. B **10**, 1400 (1974).
[25]S. Ciraci and I. P. Batra, Phys. Rev. B **15**, 4923 (1977).
[26]S. T. Pantelides and W. A. Harrison, Phys. Rev. B **13**, 2667 (1976).
[27]P. M. Schneider and W. B. Fowler, Phys. Rev. Lett. **36**, 425 (1976); Phys. Rev. B **18**, 7122 (1978).
[28]E. Calabrese and W. B. Fowler, Phys. Rev. B **28**, 1061 (1983).
[29]J. K. Rudra and W. B. Fowler, Phys. Rev. B **28**, 1061 (1983).
[30]J. R. Chelikowsky and M. Schlüter, Phys. Rev. B **15**, 4020 (1977); Solid State Commun. **21**, 381 (1977).
[31]W. Y. Ching, Phys. Rev. Lett. **46**, 607 (1981); Phys. Rev. B **26**, 6610 (1982); **26**, 6622 (1982); **26**, 6633 (1982). Band-structure calculations have also been performed recently on the other crystalline forms of $SiO_2$. See Y. P. Li and W. Y. Ching, Phys. Rev. B **31**, 2172 (1985).
[32]D. Henderson, J. Non-Cryst. Solids **16**, 1 (1974); D. Henderson and F. Herman, *ibid.* **8-10**, 359 (1972).
[33]L. Guttman, Bull. Am. Phys. Soc. **22**, 64 (1977).
[34]P. Steinhardt, R. Alben, and D. Weaire, J. Non-Cryst. Solids **15**, 199 (1974).
[35]P. N. Keating, Phys. Rev. **145**, 637 (1966).
[36]R. B. Laughlin, J. D. Joannopoulos, and D. J. Chadi, Phys. Rev. B **20**, 5228 (1979); **21**, 5733 (1980).
[37]E. Martinez and F. Ynduráin, Phys. Rev. B **24**, 5718 (1981).
[38]V. Heine, in *Solid State Physics,* edited by F. Seitz, D. Turnbull, and H. Ehrenreich (Academic, New York, 1980), Vol. 35, p. 1; R. Haydock, *ibid.*, p. 216; M. J. Kelley, *ibid.*, p. 296.
[39]E. Kauffer, P. Pecheur, and M. Gerl, Phys. Rev. B **8**, 4107 (1977).
[40]J. C. Slater and G. F. Koster, Phys. Rev. **94**, 1498 (1954).
[41]E. P. O'Reilly and J. Robertson, Phys. Rev. B **27**, 3780 (1983).
[42]R. J. Bell and P. Dean, Philos. Mag. **25**, 1381 (1972).
[43]R. L. Mozzi and B. E. Warren, J. Appl. Crystallogr. **2**, 164 (1969).
[44]N. V. Doan, Philos. Mag. A **49**, 683 (1984).
[45]W. R. Busing, J. Chem. Phys. **57**, L3008 (1972).
[46]S. K. Mitra, Philos. Mag. B **45**, 529 (1982).
[47]T. F. Soules, J. Non-Cryst. Solids **49**, 29 (1982).
[48]L. V. Woodcock, C. A. Angell, and P. A. Cheeseman, J. Chem. Phys. **65**, 1565 (1976).
[49]B. K. Chakraverty, in *Congrès International sur les couches minces, Cannes, 1970* (Société Française des Ingénieurs et Techniciens du Vide, Paris, 1970), p. 427.
[50]D. Brust, Phys. Rev. Lett. **23**, 1232 (1969).
[51]L. W. Hobbs and M. R. Pascucci, J. Phys. (Paris) Colloq. **41**, C6-237 (1980).
[52]R. P. Gupta and A. J. Freeman, Phys. Rev. Lett. **36**, 1194 (1976).
[53]In the pseudopotential calculation of Chelikowsky and Schlüter,[30] the wave function is expressed in a basis of plane waves and is not made *a priori* orthogonal to the core states. The orthogonalization is included only for the purpose of calculating the matrix elements. It is possible that the lack of properly orthogonalized wave functions leads to errors in the calculated matrix elements.
[54]T. M. Donovan and W. E. Spicer, Phys. Rev. Lett. **21**, 1572 (1968).